Genetic Analyses Reveal Functions for MAP2K3 and MAP2K6 in Mouse Testis Determination 1

Authors: Warr, Nick, Siggers, Pam, Carré, Gwenn-Aël, Wells, Sara, and Greenfield, Andy

Source: Biology of Reproduction, 94(5)

Published By: Society for the Study of Reproduction

URL: https://doi.org/10.1095/biolreprod.115.138057

BIOLOGY OF REPRODUCTION (2016) **94**(5):103, 1–7
Published online before print 23 March 2016.
DOI 10.1095/biolreprod.115.138057

Genetic Analyses Reveal Functions for MAP2K3 and MAP2K6 in Mouse Testis Determination[1]

Nick Warr,[3] Pam Siggers,[3] Gwenn-Aël Carré,[3] Sara Wells,[4] and Andy Greenfield[2,3]

[3]*Mammalian Genetics Unit, Medical Research Council, Harwell, Oxfordshire, United Kingdom*
[4]*The Mary Lyon Centre, Medical Research Council, Harwell, Oxfordshire, United Kingdom*

ABSTRACT

Testis determination in mammals is initiated by expression of *SRY* in somatic cells of the embryonic gonad. Genetic analyses in the mouse have revealed a requirement for mitogen-activated protein kinase (MAPK) signaling in testis determination: targeted loss of the kinases MAP3K4 and p38 MAPK causes complete XY embryonic gonadal sex reversal. These kinases occupy positions at the top and bottom level, respectively, in the canonical three-tier MAPK-signaling cascade: MAP3K, MAP2K, MAPK. To date, no role in sex determination has been attributed to a MAP2K, although such a function is predicted to exist. Here, we report roles for the kinases MAP2K3 and MAP2K6 in testis determination. C57BL/6J (B6) embryos lacking MAP2K3 exhibited no significant abnormalities of testis development, whilst those lacking MAP2K6 exhibited a minor delay in testis determination. Compound mutants lacking three out of four functional alleles at the two loci also exhibited delayed testis determination and transient ovotestis formation as a consequence, suggestive of partially redundant roles for these kinases in testis determination. Early lethality of double-knockout embryos precludes analysis of sexual development. To reveal their roles in testis determination more clearly, we generated *Map2k* mutant B6 embryos using a weaker *Sry* allele (Sry^{AKR}). Loss of *Map2k3* on this highly sensitized background exacerbates ovotestis development, whilst loss of *Map2k6* results in complete XY gonadal sex reversal associated with reduction of *Sry* expression at 11.25 days postcoitum. Our data suggest that MAP2K6 functions in mouse testis determination, via positive effects on *Sry,* and also indicate a minor role for MAP2K3.

disorders of sex development (DSD), MAP2K, MAP2K3, MAP2K6, MAP3K4, MAPK signaling, mouse genetics, mouse models, p38 MAPK, sex determination, sex reversal, testis development

INTRODUCTION

The sequential activation of kinases by phosphorylation is a common mechanism of signal transduction. Mitogen-activated protein kinase (MAPK)-signaling cascades are activated by a plethora of stimuli, control a number of critical cellular processes, and are characterized by three tiers of kinases that sequentially activate each other: MAP3K, MAP2K, and MAPK [1]. The number of kinases in this large family at all levels makes comprehensive genetic studies daunting. For example, there are 21 characterized MAP3Ks that activate MAP2Ks [2] and the p38 family of MAPKs alone has four members encoded by distinct genes: *Mapk14* (p38α), *Mapk11* (p38β), *Mapk12* (p38γ), and *Mapk13* (p38δ). Nevertheless, the analysis of mouse mutants lacking MAPKs, either individually or in combination, is revealing the breadth of physiological roles supported by these enzymes [3]. The range of specific phenotypes exhibited by MAPK-deficient mutants is, perhaps, surprising given the reputation that MAPKs have as housekeeping proteins performing basic cellular roles first identified in vitro.

We have recently described a requirement for MAPK signaling in mouse sex determination—the process by which the bipotential embryonic gonad becomes committed to either the testicular or ovarian pathway of development. Loss of MAP3K4 causes gonadal sex reversal in C57BL/6J (B6) XY embryos associated with disruption to the spatiotemporal expression profile of the Y-linked testis-determining gene, *Sry* [4], whilst transgenic gain of MAP3K4 function can rescue sex reversal caused by *Sry* dysregulation [5]. The activity of MAP3K4 in embryonic gonadal somatic cells is positively regulated by GADD45γ; loss of *Gadd45g* also causes XY gonadal sex reversal, which is associated with a delay in *Sry* expression [6]. Loss of MAP3K4 or GADD45γ results in reduction in the levels of activated p38 MAPK and, consistent with this observation, simultaneous genetic ablation of both *Mapk14* (p38α) and *Mapk11* (p38β) also causes XY gonadal sex reversal. Thus, a GADD45γ-MAP3K4-p38α/β MAPK pathway acts to ensure timely expression of *Sry* during the period of sex determination and prevents ovary-determining genes from exerting their effects [6, 7].

Despite these advances, we remain ignorant of which molecules at the MAP2K level of the phospho-relay module play a role in testis determination. There are seven MAP2Ks (also known as MKKs), and MAP2K3, MAP2K6, and MAP2K4 are all reported to activate p38 MAPK in different contexts [8], with reported differences in the activation of distinct p38 MAPK isoforms by MAP2K3 and MAP2K6 [9]. A number of strands of evidence support a focus on MAP2K3 and MAP2K6 function in the context of sex determination. First, these MAP2Ks are jointly implicated in activation of p38 MAPK in a number of physiological contexts, including invasion and migration of breast epithelial cells [10], T-cell apoptosis [11], cytokine stimulated fibroblast-like synoviocytes [12], neutrophil migration [13], and cisplatin resistance in non-small cell lung carcinoma [14]. Second, MAP2K3 and MAP2K6 can specifically activate p38α signaling [15]. Third, a related GADD45β-MAP3K4-MAP2K3/MAP2K6-p38

[1]This research was supported by the UK Medical Research Council through Core funding to A.G. at its Mammalian Genetics Unit, Harwell (MC_U142684167).
[2]Correspondence: Andy Greenfield, MRC Mammalian Genetics Unit, Harwell, Oxfordshire OX11 0RD, UK. E-mail: a.greenfield@har.mrc.ac.uk

Received: 22 December 2015.
First decision: 4 January 2016.
Accepted: 8 March 2016.

eISSN: 1529-7268 http://www.biolreprod.org
ISSN: 0006-3363

MAPK pathway regulates *Col10a1* transcription in terminally differentiating chondrocytes [16].

We examined sexual development in mouse embryos homozygous for null alleles of *Map2k3* or *Map2k6*. On the B6 genetic background, there are no detectable consequences after the loss of MAP2K3; loss of MAP2K6 results in a very small but consistent delay in testis determination as evidenced by ectopic expression of the meiotic entry germ cell marker, *Stra8*. Embryonic lethality precludes the analysis of sexual development in doubly homozygous *Map2k3*/*Map2k6* embryos. So, we employed a highly sensitized genetic background (B6.Y^{AKR}) to reveal the distinct contributions these kinases make to testis determination. Whilst loss of MAP2K3 exacerbates ovotestis formation in B6.Y^{AKR} embryos, loss of MAP2K6 causes complete XY gonadal sex reversal associated with reduced *Sry* expression at around 11.5 days postcoitum (dpc). Our data suggest that MAP2K6 is part of a signaling cascade, including MAP3K4 and p38 MAPK, which is required for the normal spatiotemporal expression profile of *Sry*. Our data also reveal a minor role for MAP2K3 in this process.

MATERIALS AND METHODS

Mouse Strains Used and Genotyping

All animal experimentation was approved by the Animal Welfare and Ethical Review Body at MRC Harwell and conducted in accordance with the Society for the Study of Reproduction's specific guidelines and standards. Mice used in this study were bred by license under the Animals (Scientific Procedures) Act with approval from the U.K. Home Office (PPL 30/2877). Mice were housed in individually ventilated cages in a specific opportunistic pathogen-free environment. Further details of micro- and macro-environmental conditions are available on request. Adult mice were humanely euthanized by dislocation of the neck, confirmed by palpation, and embryos were decapitated in ice-cold, phosphate-buffered saline solution.

Adult mice and embryos were sexed by a PCR assay that simultaneously amplifies the *Ube1y1* and *Ube1x* genes, using the following primer pair: 5′-TGGATGGTGTGGCCAATG-3′ and 5′-CACCTGCACGTTGCCCTT-3′ [17]. Mice harboring targeted null alleles for *Map2k3*^{tm1Flv} [18] and *Map2k6*^{tm1Flv} [11] were purchased from Jackson Laboratory. Both these null alleles encode proteins lacking catalytic domains essential for activity. Mice were maintained on the C57BL/6J (B6) background. The *Map3k4*^{tm1Flv} targeted allele and detection of the Y^{AKR} chromosome have been previously described [4].

Generation of Embryos and Expression Analyses

Noon on the day of the copulatory plug was counted as 0.5 dpc. Embryos were staged accurately based on the number of tail somites (ts) or limb and gonad morphology. Wholemount in situ hybridization (WMISH) analysis of embryonic tissues was performed as previously described [4]. Probes for *Sox9* [19], *Sry* [20], and *Stra8* [4, 21] have been previously described. WMISH was performed on at least three independent gonad samples from each embryonic class. Probes for *Map2k3* and *Map2k6* were generated by amplification of the 3′ untranslated region (3′UTR) and coding sequences from gonadal cDNA, using the following forward and reverse primers: *Map2k3* 3′UTR (5′-TCTGCCAGCATCCATACATC-3′ and 5′-GGTGGTAACCA GAGGCTGTC-3′); *Map2k3* coding (5′-GGATATCCTGCGTGTCCAAG-3′ and 5′-AGCCAGCATCCATTGTCTTT-3′); *Map2k6* 3′UTR (5′-TGGTCGACCCTACTGTGGAT-3′ and 5′-CAGCCATGAGAGCTGCAAG-3′); *Map2k6* coding (5′-AACAGCCTCAGACCAGTTCC-3′ and 5′-AG GAGCCATGTATGGTTTGC-3′). These probes gave identical results in respect to both genes.

Quantitative Reverse Transcription Polymerase Chain Reaction

Quantitative RT-PCR analyses of gene expression were performed as previously described [5]. Briefly, total RNA was extracted from gonadal tissue using an RNeasy plus micro kit (Qiagen). Two-hundred and fifty nanograms of RNA was reverse transcribed, and quantitative RT-PCR was performed using a 7500 Fast Real-Time PCR system (Applied Biosystem). At least three samples for each genotype were analyzed. Primer sequences are available on request.

Immunohistochemistry

Antibodies to the following proteins were utilized in this study: FOXL2 (a kind gift from Dagmar Wilhelm and Peter Koopman [22]), AMH (sc28912; Santa Cruz), and SRY (a kind gift from Makoto Tachibana [23]). Immunostaining was performed on sectioned, paraffin wax-embedded tissue from two independent gonad samples using the above primary antibodies (1:100) and Alexa Fluor 594 (AMH) or 488 (FOXL2, SRY) conjugated secondary antibodies (1:200). Images were captured using a Zeiss 710 multiphoton microscope.

RESULTS

Map2k3 *and* Map2k6 *Are Expressed in the Embryonic Gonad*

Expression of *Map2k3* and *Map2k6* has previously been reported in the somatic supporting cell lineage of XX and XY gonads at 11.5 dpc after microarray expression profiling [24]. We examined the embryonic gonadal expression of *Map2k3* and *Map2k6* using WMISH at the sex-determining stage of 11.5 dpc (17–18 ts stage) (Fig. 1). *Map2k3* expression was detected in the gonad and mesonephros; expression in the mesonephros was higher in the Wolffian duct (Fig. 1A). *Map2k6* expression was detected in the gonad and mesonephros at 11.5 dpc, with levels appearing higher in the mesonephros (Fig. 1B). Quantitative RT-PCR analyses of subdissected gonadal tissue at 11.5 dpc revealed expression of *Map2k3* and *Map2k6* in XX and XY wild-type embryos (Fig. 1C); *Map2k3* expression in XX gonads is higher than XY gonads by a small, but significant, amount. The expression of both genes was confirmed by comparison of wild-type and mutant gonadal tissue, revealing absence of expression of both genes in mutant gonads (Fig. 1, D and E).

Analyses of Mutant Embryos on the C57BL/6J (B6) Background Reveal Subtle Defects in Map2k6-Deficient Gonads

In order to test whether MAP2K3 and MAP2K6 function in mouse testis determination, we examined sexual development in B6 XY embryos homozygous for a *Map2k3*-targeted null allele (*Map2k3*^{tm1Flv}, henceforth *Map2k3*$^{-}$) or a *Map2k6* null (*Map2k6*^{tm1Flv}, henceforth *Map2k6*$^{-}$). Morphological examination and marker analysis at 14.5 dpc with the Sertoli cell marker *Sox9* and the ovary-specific meiotic germ cell marker *Stra8* revealed no abnormalities of gonad development in embryos lacking *Map2k3* (Fig. 2A). Embryos lacking *Map2k6* exhibited no overt abnormalities apart from a very small patch of *Stra8*-positive cells at one pole of the mutant gonad that is not present in XY wild-type controls (Fig. 2B). This abnormality was subtle but consistent. It may reflect a very brief delay in initiating testis determination in *Map2k6*-deficient embryos because, in other contexts, delayed testis determination, at least in part due to delayed *Sry* expression, is associated with *Stra8*-positive cells at the poles of XY gonads at 14.5 dpc [5]. Consistent with such a delay, *Map2k6*-deficient XY gonads at 14.5 dpc also contained a number of FOXL2-positive cells at one pole exhibiting nuclear staining (Fig. 2C). FOXL2 normally marks ovarian granulosa cells at this stage [22], suggesting that a small number of somatic cells in these XY mutant gonads have undergone sex reversal.

In order to address whether *Map2k3* compensates for the absence of *Map2k6,* we generated XY embryos lacking both copies of *Map2k6* and one copy of *Map2k3* (*Map2k3*$^{+/-}$,

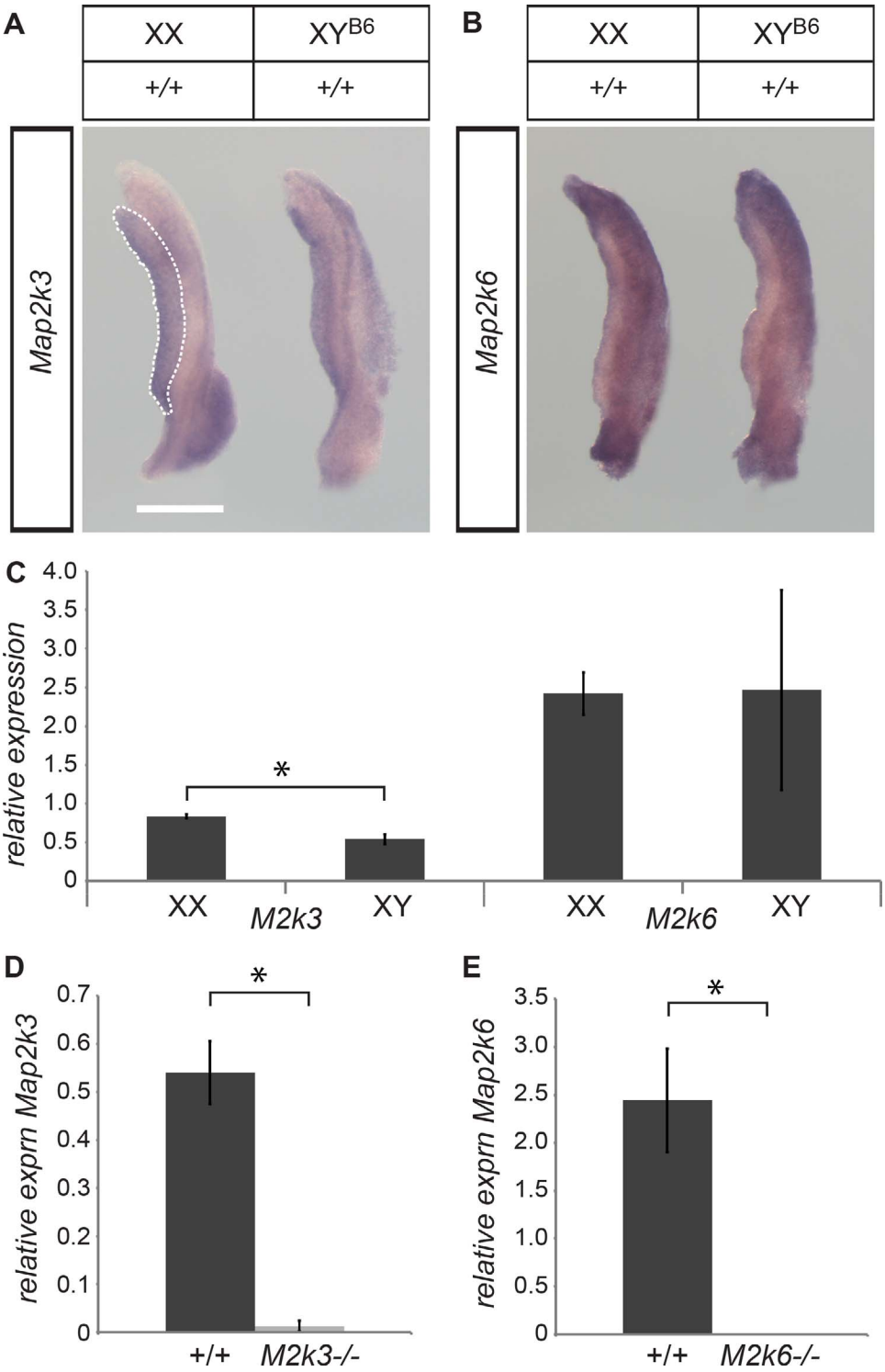

FIG. 1. *Map2k3* and *Map2k6* are expressed in the developing mouse gonad at the sex-determining stage. **A**) Wholemount in situ hybridisation (WMISH) at 11.5 dpc showing *Map2k3* expression in the gonad (area within the white dotted lines) and, to a lesser extent, the adjacent mesonephros, with prominent expression in the Wolffian duct. No sexual dimorphism is evident. Bar = 500 μm. **B**) WMISH at 11.5 dpc showing widespread expression of *Map2k6* in the developing gonad and mesonephros, with stronger signal detected in the mesonephros. **C**) Comparison of expression of *Map2k6* and *Map2k3* in XY and XX wild-type gonads. *Map2k3* expression in XX gonads is higher than XY gonads by a small, but significant, amount. Error bars throughout show standard error of the mean; $*P < 0.05$. **D**) Quantitative RT-PCR was performed using primers that amplify exonic sequences that are deleted in the *Map2k3* null allele. Expression detectable in wild-type gonads is all but absent in gonads from MAP2K3-deficient embryos, validating the specificity of the expression measurement. **E**) Quantitative RT-PCR was performed using primers that amplify exonic sequences that are deleted in the *Map2k6* null allele. Expression detectable in wild-type gonads is absent in gonads from MAP2K6-deficient embryos. RNA expression levels were normalized to those of *Hprt1* using the ΔΔCt method. Error bars show standard error of the mean.

Map2k6$^{-/-}$) (Fig. 2D). These compound mutants exhibited pronounced abnormalities of testis development at 14.5 dpc. Testis cord morphology was noticeably less well defined in comparison to littermate controls, and clumps of *Stra8*-positive

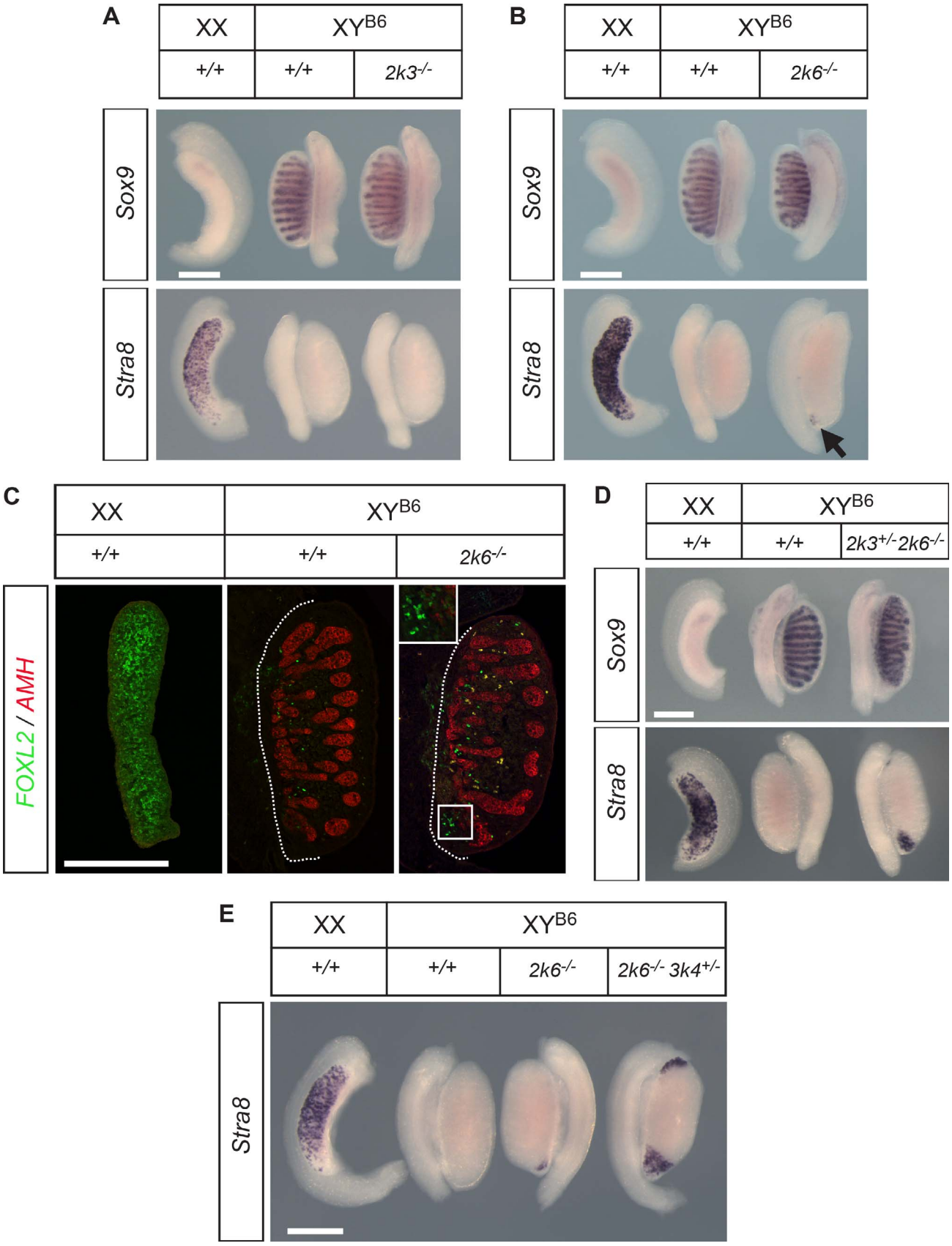

FIG. 2. Characterization of gonadal phenotypes at 14.5 dpc in B6 embryos lacking MAP2K3 and MAP2K6. **A**) WMISH of *Sox9* and *Stra8* in gonads from MAP2K3-deficient embryos reveals no overt abnormalities. Bar = 500 μm. **B**) WMISH of *Sox9* and *Stra8* in gonads from MAP2K6-deficient embryos reveals a small but consistent patch of *Stra8* expression (arrow) at one pole of the mutant gonad. Bar = 500 μm. **C**) Immunostaining of gonadal tissue sections comparing MAP2K6-deficient B6 XY embryos and wild-type controls with the Sertoli cell marker AMH (red) and granulosa cell marker FOXL2 (green) reveals a small cluster of FOXL2-positive cells at the caudal pole of the mutant ($2k6^{-/-}$) gonad (white box) exhibiting nuclear staining (see higher

cells, sometimes quite large, were detected at one or both poles of compound mutant gonads (Fig. 2D). These data suggest disruption to testis determination by a further delay in its initiation and propagation to the gonadal poles caused by the additional loss of one copy of *Map2k3*.

A previous study of the role of GADD45γ and MAP3K4 in testis determination showed that B6 XY embryos heterozygous for a *Map3k4* null allele form normal testes at 14.5 dpc, apart from a very small patch of *Stra8* expression at one pole (see Fig. 4 of [6]), reminiscent of *Map2k6*-deficient gonads at the same stage. We generated embryos combining these two genotypes (*Map2k6*$^{-/-}$, *Map3k4*$^{+/-}$). At 14.5 dpc, gonads of this genotype had regions of *Stra8* expression at their poles that were much more extensive than either *Map2k6*$^{-/-}$ or *Map3k4*$^{+/-}$ gonads alone (Fig. 2E). These data confirm a role for *Map2k6* in testis determination and also reveal genetic interaction between *Map2k6* and *Map3k4* consistent with a role for these two genes in the same testis-determining pathway.

Loss of MAP2K6 on the Highly Sensitized B6.Y^{AKR} Background Causes XY Gonadal Sex Reversal

We predicted that doubly homozygous (*Map2k3*$^{-/-}$, *Map2k6*$^{-/-}$) embryos would exhibit much more severe disruptions to testis determination, but examination of testis development in these double homozygotes was precluded by lethality at around 11.5 dpc [25]. In order to examine and compare the distinct contributions made by *Map2k3* and *Map2k6* to testis determination on the same genetic background, we bred the null alleles on to B6.Y^{AKR}, a background that is highly sensitized to disruptions to testis determination [26]. Whilst B6.Y^{AKR} mice develop as normal males, embryonic gonad development is characterized by delayed testis determination and transient ovotestis formation as a consequence. This is associated, at least in part, with a delay in peak expression of the *Mus domesticus Sry* allele, *Sry*^{AKR}, on the B6 background at the onset of testis determination [5, 27].

Embryos lacking *Map2k3* on the B6.Y^{AKR} background had ovotestes at 14.5 dpc (Fig. 3A). *Sox9* expression is detectable in central cords with an irregular morphology, but is lacking from one or both poles, whilst *Stra8* expression is prominent in the polar regions of these ovotestes (Fig. 3A). Control B6.Y^{AKR} gonads also exhibit polar *Stra8* expression as expected, although there was a tendency for the extent of *Stra8* expression to be greater in *Map2k3*-deficient mutants than in controls (Fig. 3A and data not shown), and the most severely affected gonads were from homozygous mutant embryos. Thus, the disruptive impact of *Map2k3* deletion on testis determination is difficult to quantify but is significant.

In contrast to this, B6.Y^{AKR} embryos lacking *Map2k6* exhibited complete gonadal sex reversal, as evidenced by gonadal morphology, absence of *Sox9* expression (Fig. 3B), and high levels of *Stra8* (Fig. 3B) and FOXL2 (Fig. 3C) throughout the gonad at 14.5 dpc. Complete sex reversal was also seen in *Map2k3*$^{+/-}$, *Map2k6*$^{-/-}$ compound mutants (Fig. 3B). Interestingly, B6.Y^{AKR} embryos lacking just a single copy of *Map2k6* occasionally developed ovotestes with substantial amounts of *Stra8*-positive tissue (Fig. 3B and data not shown). These data clearly indicate a requirement for *Map2k6* function in testis determination; additionally, a minor role for *Map2k3* is suggested by these data. Such a minor role is also supported by the subtle increase in severity of gonadal phenotype in *Map2k3*$^{+/-}$, *Map2k6*$^{-/-}$ embryos on the B6 background when compared to *Map2k6*$^{-/-}$ (Fig. 2D).

Sry *Expression Is Disrupted in* Map2k6$^{-/-}$ *Gonads on B6.Y^{AKR}*

Given the link between *Map3k4* expression and *Sry* expression in both loss- and gain-of-function mouse models [4, 5], and the positive link between p38 MAPK activity and *Sry* [6, 28], we examined *Sry* expression in embryonic gonads lacking *Map2k6* on the B6.Y^{AKR} background at the early stage of 11.25 dpc (16 ts) using WMISH (Fig. 3D). A clear reduction in *Sry* signal was observed in mutant gonads when compared to stage-matched wild-type controls, consistent with the observed XY gonadal sex reversal in this strain. Similarly, detection of SRY protein in wild-type and mutant gonads at the 17 ts stage using immunostaining revealed a greatly reduced number of SRY-positive cells in mutant gonads and lower levels of SRY protein in those cells (Fig. 3E).

DISCUSSION

Our data reveal roles for MAP2K6 and MAP2K3 in mouse testis determination. The use of the sensitized B6.Y^{AKR} background reveals a differential sensitivity to loss of these two MAP2Ks, with testis determination being completely disrupted by the loss of MAP2K6. In contrast, loss of MAP2K3 merely exacerbates ovotestis formation on this background. The loss of either protein on the standard B6 background results in a negligible, but consistent, phenotype only in the case of MAP2K6, with mutant gonads exhibiting a very small cluster of *Stra8*-positive cells at the caudal pole and FOXL2-positive cells at the same pole. The expansion of the *Stra8*-positive region in embryos lacking an additional copy of *Map2k3* (*Map2k3*$^{+/-}$, *Map2k6*$^{-/-}$) demonstrates that these proteins act redundantly during testis determination. However, this phenotype is still relatively modest. It was not possible to examine embryos lacking all copies of *Map2k3* and *Map2k6*. Regardless of the phenotypic outcome of such an experiment, our data do not exclude roles for other MAP2Ks in testis determination.

Conditional gene targeting would allow the generation of mice lacking both MAP2K3 and MAP2K6 in gonadal somatic cells, and our prediction is that severe disruption to testis determination would ensue, perhaps similar to the phenotype caused by loss of *Map2k6* alone on B6.Y^{AKR}. Clearly, it would also be interesting to investigate the gonadal phenotypes of embryos lacking MAP2K4 and MAP2K7, but simultaneous removal of multiple MAP2Ks (greater than two) from the developing gonad would be practically impossible using conventional conditional gene targeting, though possible using recently developed genome editing tools [29].

We infer from our data, described here and elsewhere, the existence of a GADD45γ/MAP3K4/MAP2K3/6/p38 MAPK signaling pathway required for normal expression of *Sry* in

magnification image in inset). A large number of fluorescent cells in the interstitium of the mutant gonad are blood cells. The occasional interstitial cell can also be seen exhibiting nuclear staining, but these rare cells are also observed in wild-type control gonads and are of unknown significance. The dotted line indicates the border between the gonad (right) and mesonephros (left). Bar = 500 μm. **D**) Compound mutant embryos (*Map2k3*$^{+/-}$, *Map2k6*$^{-/-}$) have gonads exhibiting a larger area of *Stra8* expression at one pole, indicating some redundancy between MAP2K3 and MAP2K6 function during testis determination. Bar = 500 μm. **E**) WMISH reveals more extensive regions of *Stra8* expression at the gonadal poles in compound mutants (*Map2k6*$^{-/-}$, *Map3k4*$^{+/-}$) when compared to littermates only lacking *Map2k6* (*Map2k6*$^{-/-}$). Bar = 500 μm.

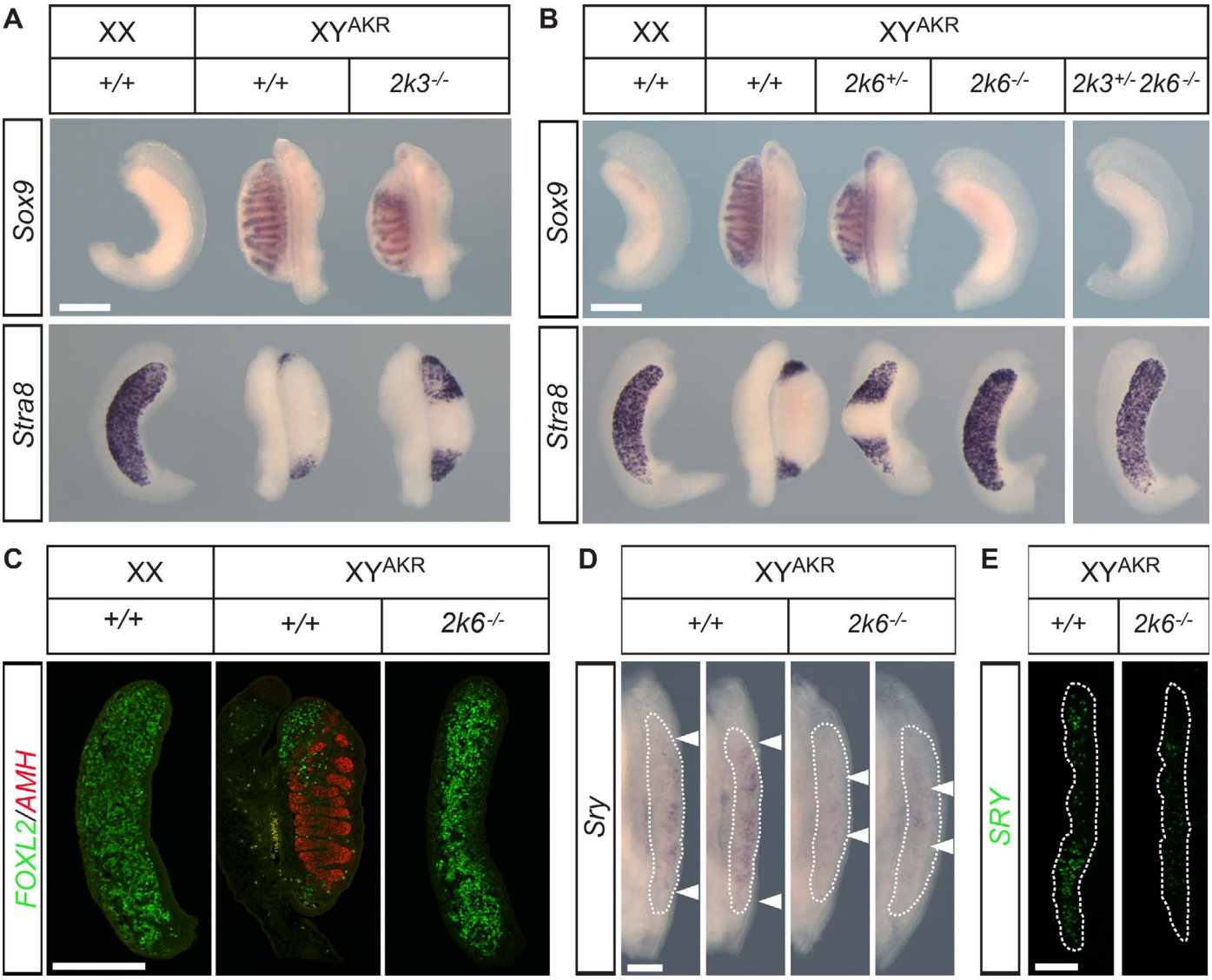

FIG. 3. Gonadal sex reversal phenotype at 14.5 dpc in MAP2K6-deficient embryos on the B6.Y^{AKR} background. **A**) WMISH with *Sox9* and *Stra8* probes showing loss of *Sox9* signal, abnormal cord morphology, and extensive expression of *Stra8* in *Map2k3* null mutant gonads compared to wild-type controls. Control XY gonads (center, lower panel) exhibit small *Stra8*-positive regions due to transient ovotestis formation associated with the reduced functionality of the *Sry*^{AKR} allele on B6. Bar = 500 μm. **B**) WMISH with *Sox9* and *Stra8* probes reveals complete gonadal sex reversal in *Map2k6*-deficient gonads and compound mutant gonads (*Map2k3*$^{+/-}$, *Map2k6*$^{-/-}$), associated with overt ovarian morphology, loss of *Sox9,* and ectopic *Stra8* expression throughout. Heterozygous mutant gonads (*Map2k6*$^{+/-}$) may also exhibit large *Stra8*-positive regions and reduced *Sox9* expression at the poles and abnormal cord morphology, in contrast to wild-type controls. Bar = 500 μm. **C**) Immunostaining of gonadal tissue sections comparing MAP2K6-deficient embryos and wild-type controls. AMH (red) is detected in testis cords of control gonads but is absent from mutant gonads. The ovarian granulosa cell marker FOXL2 (green) is detected throughout the XY mutant gonad, as it is in XX controls. Some polar FOXL2 is detected in the B6.Y^{AKR} wild-type control for reasons explained above. Bar = 500 μm. **D**) WMISH at 11.25 dpc with an *Sry* probe shows clear expression throughout the gonad (area within white dotted lines; limits of expression indicated by arrowheads) in two B6.Y^{AKR} wild-type (+/+) controls; but signal is negligible and restricted to central regions (indicated by arrowheads) in two MAP2K6-deficient gonads (*2k6*$^{-/-}$) on the same background at exactly the same stage (16 ts). Bar = 200 μm. **E**) Immunostaining with an anti-SRY antibody at 17 ts reveals a large number of SRY-positive cells in the control (+/+) gonad (area within white dotted line), but few SRY-positive cells in a stage-matched mutant (*2k6*$^{-/-}$) gonad. Bar = 200 μm.

gonadal somatic cells and, as a consequence, testis determination. The genetic interaction data reported here support roles for MAP3K4 and MAP2K6 in the same testis-determining pathway. However, we do not rule out other pathways containing MAP2K3/MAP2K6. We have previously reported evidence that GATA4, a known regulator of *Sry* expression, is a target of GADD45γ/MAP3K4/p38 MAPK signaling. MAPKs are increasingly associated with diverse regulatory functions mediated by their direct recruitment to chromatin [30]. Identification of additional targets of MAPK signaling in testis determination will require careful phospho-proteomic and/or epigenomic analyses of the developing gonadal soma in wild-type and mutant gonads.

The molecular basis of disorders of sex development (DSD) in the human population is still an area of intensive investigation [31]. Approaches to identifying the missing genes responsible for DSD include next-generation sequencing of exome libraries derived from unexplained cases [32, 33]. Our data concerning MAP2K3 and MAP2K6 provide a formal demonstration that MAP2Ks function in mammalian testis determination and mutations in related human genes may be the cause of unexplained cases of 46,XY DSD. We suggest that

it will be important for clinical geneticists and mouse geneticists to work closely in order to definitively establish causality for novel genetic variants associated with all cases of human DSD, especially when those variants are very rare. The mouse, with its distinct genetic backgrounds and powerful mutagenesis methodologies that allow for the careful assessment of in vivo functionality at all levels remains an excellent tool for the clinical geneticist studying DSD.

Finally, MAPK signaling cascades are associated with scaffold proteins that are thought to be important for controlling signaling dynamics with respect to spatial location, specificity, intensity, and duration [34]. A protein acting as a MAPK scaffold has not yet been shown to be required for testis determination in the mouse. Such a protein, and others supporting signal transduction in early gonad development, if identified, will also permit further investigation into the molecular mechanisms by which signals control gonadal cell fate.

ACKNOWLEDGMENT

We thank the staff of the Mary Lyon Centre (MLC) at Harwell for animal husbandry support, in particular Jackie Harrison, Lee Kent, and Alison Gallop in Ward 5. We thank Dagmar Wilhelm (University of Melbourne, Australia) for kindly providing anti-FOXL2 antibody and Makoto Tachibana (Kyoto University, Japan) for kindly providing anti-SRY antibody. We thank the staff of the MLC histology facility for sectioning, the staff of the GEMS facility for genotyping, and Martin Fray and his staff in the FESA Core for line rederivations.

REFERENCES

1. Rubinfeld H, Seger R. The ERK cascade as a prototype of MAPK signaling pathways. Methods Mol Biol 2004; 250:1–28.
2. Craig EA, Stevens MV, Vaillancourt RR, Camenisch TD. MAP3Ks as central regulators of cell fate during development. Dev Dyn 2008; 237: 3102–3114.
3. Aouadi M, Binetruy B, Caron L, Le Marchand-Brustel Y, Bost F. Role of MAPKs in development and differentiation: lessons from knockout mice. Biochimie 2006; 88:1091–1098.
4. Bogani D, Siggers P, Brixey R, Warr N, Beddow S, Edwards J, Williams D, Wilhelm D, Koopman P, Flavell RA, Chi H, Ostrer H, et al. Loss of mitogen-activated protein kinase kinase kinase 4 (MAP3K4) reveals a requirement for MAPK signalling in mouse sex determination. PLoS Biol 2009; 7:e1000196.
5. Warr N, Siggers P, Carre GA, Bogani D, Brixey R, Akiyoshi M, Tachibana M, Teboul L, Wells S, Sanderson J, Greenfield A. Transgenic expression of Map3k4 rescues T-associated sex reversal (Tas) in mice. Hum Mol Genet 2014; 23:3035–3044.
6. Warr N, Carre GA, Siggers P, Faleato JV, Brixey R, Pope M, Bogani D, Childers M, Wells S, Scudamore CL, Tedesco M, del Barco Barrantes I, et al. Gadd45gamma and Map3k4 interactions regulate mouse testis determination via p38 MAPK-mediated control of Sry expression. Dev Cell 2012; 23:1020–1031.
7. Carre GA, Greenfield A. Characterising novel pathways in testis determination using mouse genetics. Sex Dev 2014; 8:199–207.
8. Ono K, Han J. The p38 signal transduction pathway: activation and function. Cell Signal 2000; 12:1–13.
9. Remy G, Risco AM, Inesta-Vaquera FA, Gonzalez-Teran B, Sabio G, Davis RJ, Cuenda A. Differential activation of p38MAPK isoforms by MKK6 and MKK3. Cell Signal 2010; 22:660–667.
10. Shin I, Kim S, Song H, Kim HR, Moon A. H-Ras-specific activation of Rac-MKK3/6-p38 pathway: its critical role in invasion and migration of breast epithelial cells. J Biol Chem 2005; 280:14675–14683.
11. Tanaka N, Kamanaka M, Enslen H, Dong C, Wysk M, Davis RJ, Flavell RA. Differential involvement of p38 mitogen-activated protein kinase kinases MKK3 and MKK6 in T-cell apoptosis. EMBO Rep 2002; 3: 785–791.
12. Inoue T, Hammaker D, Boyle DL, Firestein GS. Regulation of p38 MAPK by MAPK kinases 3 and 6 in fibroblast-like synoviocytes. J Immunol 2005; 174:4301–4306.
13. Wang Q, Yerukhimovich M, Gaarde WA, Popoff IJ, Doerschuk CM. MKK3 and -6-dependent activation of p38alpha MAP kinase is required for cytoskeletal changes in pulmonary microvascular endothelial cells induced by ICAM-1 ligation. Am J Physiol Lung Cell Mol Physiol 2005; 288:L359–L369.
14. Galan-Moya EM, de la Cruz-Morcillo MA, Llanos Valero M, Callejas-Valera JL, Melgar-Rojas P, Hernadez Losa J, Salcedo M, Fernandez-Aramburo A, Ramon y Cajal S, Sanchez-Prieto R. Balance between MKK6 and MKK3 mediates p38 MAPK associated resistance to cisplatin in NSCLC. PLoS One 2011; 6:e28406.
15. Wen HC, Avivar-Valderas A, Sosa MS, Girnius N, Farias EF, Davis RJ, Aguirre-Ghiso JA. p38alpha Signaling induces anoikis and lumen formation during mammary morphogenesis. Sci Signal 2011; 4:ra34.
16. Tsuchimochi K, Otero M, Dragomir CL, Plumb DA, Zerbini LF, Libermann TA, Marcu KB, Komiya S, Ijiri K, Goldring MB. GADD45beta enhances Col10a1 transcription via the MTK1/MKK3/6/p38 axis and activation of C/EBPbeta-TAD4 in terminally differentiating chondrocytes. J Biol Chem 2010; 285:8395–8407.
17. Warr N, Siggers P, Bogani D, Brixey R, Pastorelli L, Yates L, Dean CH, Wells S, Satoh W, Shimono A, Greenfield A. Sfrp1 and Sfrp2 are required for normal male sexual development in mice. Dev Biol 2009; 326: 273–284.
18. Lu HT, Yang DD, Wysk M, Gatti E, Mellman I, Davis RJ, Flavell RA. Defective IL-12 production in mitogen-activated protein (MAP) kinase kinase 3 (Mkk3)-deficient mice. EMBO J 1999; 18:1845–1857.
19. Wright E, Hargrave MR, Christiansen J, Cooper L, Kun J, Evans T, Gangadharan U, Greenfield A, Koopman P. The *Sry*-related gene *Sox-9* is expressed during chondrogenesis in mouse embryos. Nature Genetics 1995; 9:15–20.
20. Bullejos M, Koopman P. Spatially dynamic expression of Sry in mouse genital ridges. Dev Dyn 2001; 221:201–205.
21. Warr N, Bogani D, Siggers P, Brixey R, Tateossian H, Dopplapudi A, Wells S, Cheeseman M, Xia Y, Ostrer H, Greenfield A. Minor abnormalities of testis development in mice lacking the gene encoding the MAPK signalling component, MAP3K1. PLOs One 2011; 6:e19572.
22. Wilhelm D, Washburn LL, Truong V, Fellous M, Eicher EM, Koopman P. Antagonism of the testis- and ovary-determining pathways during ovotestis development in mice. Mech Dev 2009; 126:324–336.
23. Kuroki S, Matoba S, Akiyoshi M, Matsumura Y, Miyachi H, Mise N, Abe K, Ogura A, Wilhelm D, Koopman P, Nozaki M, Kanai Y, et al. Epigenetic regulation of mouse sex determination by the histone demethylase Jmjd1a. Science 2013; 341:1106–1109.
24. Jameson SA, Natarajan A, Cool J, DeFalco T, Maatouk DM, Mork L, Munger SC, Capel B. Temporal transcriptional profiling of somatic and germ cells reveals biased lineage priming of sexual fate in the fetal mouse gonad. PLoS Genet 2012; 8:e1002575.
25. Brancho D, Tanaka N, Jaeschke A, Ventura JJ, Kelkar N, Tanaka Y, Kyuuma M, Takeshita T, Flavell RA, Davis RJ. Mechanism of p38 MAP kinase activation in vivo. Genes Dev 2003; 17:1969–1978.
26. Bouma GJ, Washburn LL, Albrecht KH, Eicher EM. Correct dosage of Fog2 and Gata4 transcription factors is critical for fetal testis development in mice. Proc Natl Acad Sci U S A 2007; 104:14994–14999.
27. Bullejos M, Koopman P. Delayed Sry and Sox9 expression in developing mouse gonads underlies B6-Y(DOM) sex reversal. Dev Biol 2005; 278: 473–481.
28. Gierl MS, Gruhn WH, von Seggern A, Maltry N, Niehrs C. GADD45G functions in male sex determination by promoting p38 signaling and Sry expression. Dev Cell 2012; 23:1032–1042.
29. Wang H, Yang H, Shivalila CS, Dawlaty MM, Cheng AW, Zhang F, Jaenisch R. One-step generation of mice carrying mutations in multiple genes by CRISPR/Cas-mediated genome engineering. Cell 2013; 153: 910–918.
30. Klein AM, Zaganjor E, Cobb MH. Chromatin-tethered MAPKs. Curr Opin Cell Biol 2013; 25:272–277.
31. Ohnesorg T, Vilain E, Sinclair AH. The genetics of disorders of sex development in humans. Sex Dev 2014; 8:262–272.
32. Tobias ES, McElreavey K. Next generation sequencing for disorders of sex development. Endocr Dev 2014; 27:53–62.
33. Baxter RM, Arboleda VA, Lee H, Barseghyan H, Adam MP, Fechner PY, Bargman R, Keegan C, Travers S, Schelley S, Hudgins L, Mathew RP, et al. Exome sequencing for the diagnosis of 46,XY disorders of sex development. J Clin Endocrinol Metab 2015; 100:E333–E344.
34. Witzel F, Maddison L, Bluthgen N. How scaffolds shape MAPK signaling: what we know and opportunities for systems approaches. Front Physiol 2012; 3:475.